

A UNITED STATES
DEPARTMENT OF
COMMERCE
PUBLICATION



NOAA Technical Memorandum NWS TDL-38

U.S. DEPARTMENT OF COMMERCE
National Oceanic and Atmospheric Administration
National Weather Service

Objectively Computed Surface Diagnostic Fields

ROBERT J. BERMOWITZ

Systems
Development
Office

SILVER SPRING, MD.

February 1971

NOAA TECHNICAL MEMORANDA

National Weather Service, Techniques Development Laboratory Series

The primary purpose of the Techniques Development Laboratory of the Office of Systems Development is to translate increases of basic knowledge in meteorology and allied disciplines into improved operating techniques and procedures. To achieve this goal, the Laboratory conducts and sponsors applied research and development aimed at the improvement of diagnostic and prognostic methods for producing weather information. The Laboratory performs studies both for the general improvement of prediction methodology used in the National Meteorological Service System and for the more effective utilization of weather forecasts by the ultimate user.

NOAA Technical Memoranda in the National Weather Service Techniques Development Laboratory series facilitate rapid distribution of material which may be preliminary in nature and which may be published formally elsewhere at a later date. Publications 1 to 5 are in the former series, Weather Bureau Technical Notes (TD), Techniques Development Laboratory (TDL) Reports; publications 6 to 36 are in the former series, ESSA Technical Memoranda, Weather Bureau Technical Memoranda (WBTM). Beginning with TDL 37, publications are now part of the series NOAA Technical Memoranda, National Weather Service (NWS).

Publications listed below are available from the National Technical Information Service, U.S. Department of Commerce, Sills Bldg., 5285 Port Royal Road, Springfield, Va. 22151. Price: \$3.00 paper copy; \$0.95 microfiche. Order by accession number shown in parentheses at end of each entry.

- TN 10 TDL 1 Objective Prediction of Daily Surface Temperature. William H. Klein, Curtis W. Crockett, and Carlos R. Dunn, October 1965. (PB-168 590)
- TN 11 TDL 2 Hurricane Cindy Galveston Bay Tides. N. A. Pore, A. T. Angelo, and J. G. Taylor, September 1965. (PB-168 608)
- TN 29 TDL 3 Atmospheric Effects on Re-Entry Vehicle Dispersions. Karl R. Johannessen, December 1965. (PB-169 381)
- TN 45 TDL 4 A Synoptic Climatology of Winter Precipitation from 700-mb. Lows for the Intermountain Areas of the West. D. L. Jorgensen, W. H. Klein, and A. F. Korte, May 1966. (PB-170 635)
- TN 47 TDL 5 Hemispheric Specification of Sea Level Pressure from Numerical 700-mb. Height Forecasts. William H. Klein and Billy M. Lewis, June 1966. (PB-173 091)
- WBTM TDL 6 A Fortran Program for the Calculation of Hourly Values of Astronomical Tide and Time and Height of High and Low Water. N. A. Pore and P. A. Cummings, January 1967. (PB-174 660)
- WBTM TDL 7 Numerical Experiments Leading to the Design of Optimum Global Meteorological Networks. M. A. Alaka and F. Lewis, February 1967. (PB-174 497)
- WBTM TDL 8 An Experiment in the Use of the Balance Equation in the Tropics. M. A. Alaka, D. T. Rubsam, and G. E. Fisher, March 1967. (PB-174 501)
- WBTM TDL 9 A Survey of Studies of Aerological Network Requirements. M. A. Alaka, May 1967. (PB-174 984)
- WBTM TDL 10 Objective Determination of Sea Level Pressure from Upper Level Heights. William Klein, Frank Lewis, and John Stackpole, May 1967. (PB-179 949)
- WBTM TDL 11 Short Range, Subsynchronous Surface Weather Prediction. H. R. Glahn and D. A. Lowry, July 1967. (PB-175 772)
- WBTM TDL 12 Charts Giving Station Precipitation in the Plateau States from 700-Mb. Lows During Winter. D. L. Jorgensen, A. F. Korte, and J. A. Bunce, Jr., October 1967. (PB-176 742)
- WBTM TDL 13 Interim Report on Sea and Swell Forecasting. N. A. Pore and W. S. Richardson, December 1967. (PB-177 038)
- WBTM TDL 14 Meteorological Analysis of 1964-65 ICAO Turbulence Data. DeVer Colson, September 1968. (PB-180 268)
- WBTM TDL 15 Prediction of Temperature and Dew Point by Three-Dimensional Trajectories. Ronald M. Reap, September 1968. (PB-180 727)

(Continued on inside back cover)

U.S. DEPARTMENT OF COMMERCE
National Oceanic and Atmospheric Administration
National Weather Service

NOAA Technical Memorandum NWS TDL-38

OBJECTIVELY COMPUTED SURFACE DIAGNOSTIC FIELDS

Robert J. Bermowitz



Systems Development Office
Techniques Development Laboratory

SILVER SPRING, MD.
February 1971

UDC 551.509.314(73-11)"1969.12.21"

551.5	Meteorology
.509	Synoptic analysis and forecasting
.314	Statistical and objective methods of forecasting
(73-11)	Eastern USA
"1969.12.21"	December 21, 1969

CONTENTS

	<u>Page</u>
Abstract	1
Introduction	1
Basic Analysis Technique	2
Surface Wind Analysis	2
Surface Temperature Analysis	5
Diagnostic Computations	8
Results of Computations	10
Summary and Conclusions	22
Acknowledgments	22
References	23

OBJECTIVELY COMPUTED SURFACE DIAGNOSTIC FIELDS

Robert J. Bermowitz

ABSTRACT

Hourly surface observations of temperature and wind are objectively analyzed on a grid with a gridlength of about 50 miles ($\frac{1}{2}$ that used at the National Meteorological Center). The analyses are then used to compute relatively small-scale diagnostic fields of divergence, vorticity, frontogenetical function, and temperature advection.

The results of two test cases are described. It appears that the diagnostic fields can be helpful in short range predictions. In some cases, they seem to be related to significant smaller scale features such as regions of thunderstorm and tornado activity and incipient cyclogenesis. Synoptic scale features such as frontal zones appear to be rather well represented by the diagnostic fields.

INTRODUCTION

In the area of objective weather prediction, much emphasis has recently been placed on analyzing and predicting events on the subsynoptic scale. A prime example of the research and development effort in this direction is the Subsynoptic Advection Model (SAM), developed within the Techniques Development Laboratory (TDL) and described by Glahn et al. (1969b). SAM is currently run operationally twice per day at the National Meteorological Center (NMC). The apparent superiority of sea level pressure and categorical precipitation forecasts produced by this model, compared to other machine produced forecasts, is in part due to the smaller scale analyses which are used as input to SAM.

Objective surface analyses and computed diagnostic fields, containing features on the subsynoptic scale, may also be useful tools in short period forecasting if supplied directly and frequently to the forecaster. The diagnostic fields, which are computed directly from the analyses and should be related to the concurrent weather, may be useful in situations where the low level numerical forecasts from the Primitive Equation Model (PE) (Shuman and Hovermale, 1968), SAM, and the Trajectory Model (Reap, 1968), are slow in movement or development, or lacking in detail. In the former case, the numerical guidance could be updated; in the latter, it could be detailed. The diagnostic fields might also be used as predictors in short period statistical prediction schemes.

This paper describes objective analyses of the surface wind and temperature and the kinematically computed fields of divergence, vorticity, frontogenetical function, and temperature advection as related to the observed weather.

Of course, the surface wind and temperature observations contain considerable local variation. As a result, the analyses and subsequent diagnostic fields obtained from these data include small-scale features that are not related to significant weather. The major problem is to remove most of the local variability from the analyses and computations, while leaving intact as much of the pertinent weather-related detail as possible.

BASIC ANALYSIS TECHNIQUE

The analysis area used (figure 1) contains a 39x40 grid with a space scale of 95 km at 60° N. ($\frac{1}{2}$ NMC gridlength). For the most part, the land area is characterized by a relatively dense network of observations; in contrast, no data are obtained over the ocean areas.

The program for automatically decoding the hourly airways observations, developed within TDL by Hollenbaugh et al. (1969), is used to obtain the initial data. These data are then analyzed by a technique based on the method of Bergthórssen and Døss (1955) and Cressman (1959). The program actually employed to analyze the wind and temperature is a modification of a basic analysis program designed to analyze any scalar variable. The details are described by Glahn et al. (1969a). Here, it suffices to give the particular modifications of this basic program necessary to analyze the wind and temperature data.

SURFACE WIND ANALYSIS

In the wind analysis program, the variables considered are the scalar, eastward and northward components of the wind vector. These components are analyzed consecutively on each pass over the data. At the conclusion of each pass the vector wind is computed at every gridpoint.

In this application of the basic analysis program, four data passes are made. On each cycle, the radius of influence is respectively, 8.0, 5.0, 2.5, and 1.0 grid interval.

On the first pass a type 2 correction (see Glahn et al. 1969a) is applied at every gridpoint of the first guess field, which in this case is a PE forecast of the boundary layer wind. On subsequent passes, a type 3 correction is used.

The error detecting procedure does not work very well due to the relatively large variability of the surface winds. Acceptance criteria were defined under the assumption that it is better to accept a few poor observations than to discard several good ones; subsequent smoothing reduces the effect of the erroneous data. Nevertheless, the error detecting routine has the capability of discarding obviously poor quality observations.

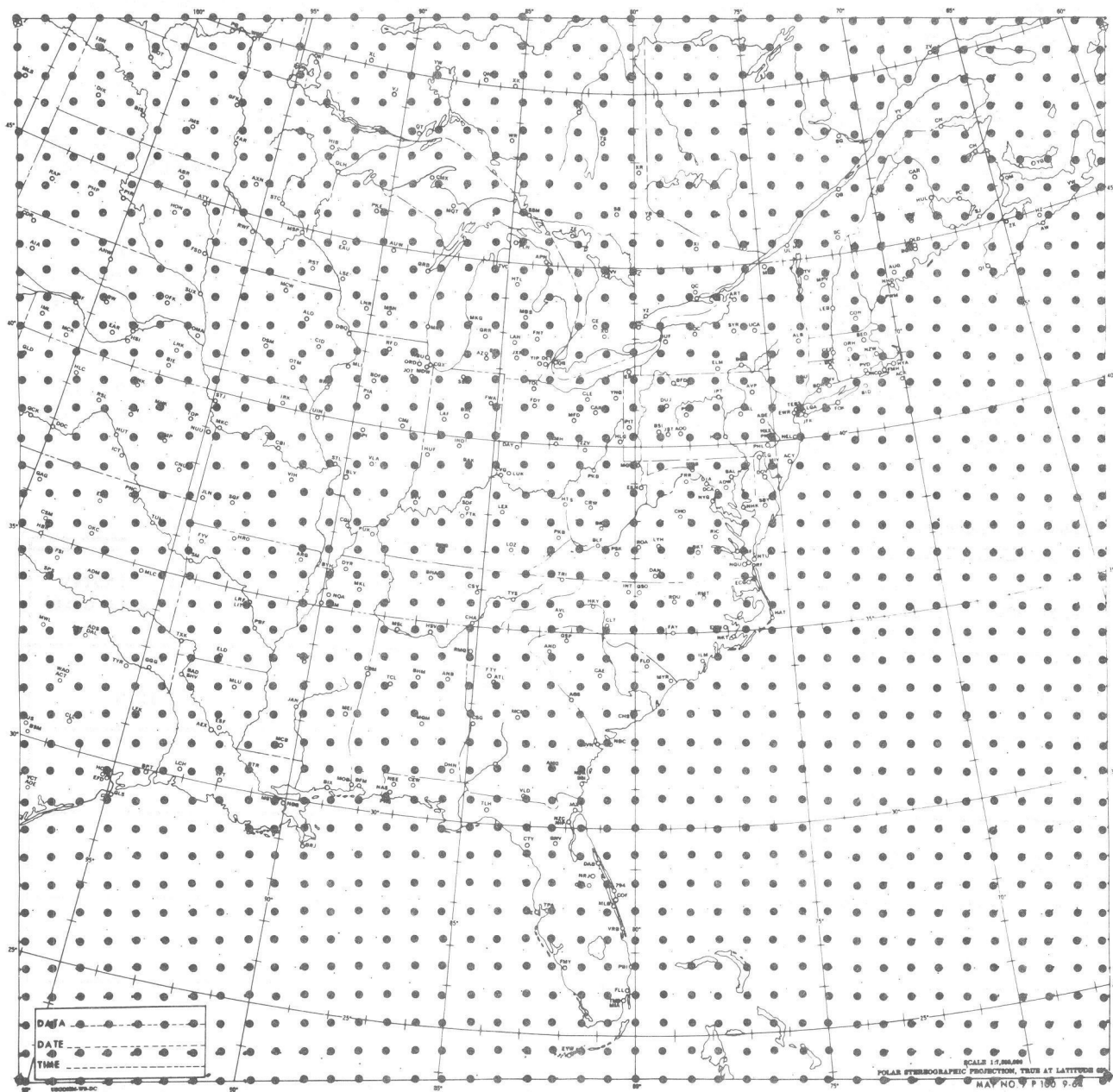


Figure 1.--The analysis and computational area, and 39 x 40 grid. The grid-length is the same as that used in SAM.

The important details of this procedure applicable to wind observations follow. On the first data pass, the "buddy system" is employed to check all observations. In this system, an observation is permanently discarded if it differs from both of its two closest neighboring observations by more than a specified amount (acceptance criteria) in either direction or speed.

On all subsequent data passes, a direction and speed check is made of every observation by comparing it to the value of the previous analysis interpolated to the location of the observation. If the station value differs from the analyzed value by more than the acceptance criteria, in either speed or direction, it is discarded for that pass only.

On all scans, the wind direction is not checked if the observed wind speed is less than or equal to 8 knots. In this case, only a speed check is made. Here, an attempt is being made to prevent those observations with the greatest variability in wind direction from being discarded.

The empirically determined acceptance criteria used on each data pass, ER1 (see Glahn et al. 1969a), and also in the buddy system check on pass 1, ER2, and ER3 are summarized in Table 1.

Table 1. Acceptance criteria used in wind analysis

PASS NO.	ER1 (degrees knots)	ER2(>8 KNOTS) (degrees knots)	ER2(<8 KNOTS) (knots)	ER3(>8 KNOTS) (degrees/grid unit) (knots/grid unit)	ER3(<8 KNOTS) (knots/grid unit)
1	166 22.7	120 12.0	10.0	120 12.0	10.0
2	179 23.5				
3	147 15.0				
4	131 11.1				

Usually, at the conclusion of each cycle, the analyzed component wind fields are smoothed. The smoother is the same as that used in the basic analysis program; the smoothing parameter b is 0.0 (no smoothing), 5.0, 1.0, and 5.0 for scans 1 through 4, respectively.

Three smoothing passes (heavy smoothing) are required at the end of pass 2 to remove a discontinuity in the analysis over the ocean area. The discontinuity develops at a distance from the coast nearly equal to the radius of influence used on this pass. It is a result of no data being used in the ocean area, as well as initial use of the more rapidly convergent type of correction.

The smoother is also applied three times over the analysis at the conclusion of the final pass. The primary purpose of the analyzed fields is to provide gridpoint information for computing diagnostic fields. In order for these fields to be of practical use, it is necessary to remove the local, non-weather related variability from the analyses. Unfortunately, it is not possible to do this without, at least partially, smoothing some of the significant variability, e.g. wind shear lines and steep temperature gradients associated with fronts.

An example of a wind analysis is shown in figure 2. This can be compared to the observed winds illustrated in figure 3. Over the ocean area, the analyzed field (not shown) is essentially the first guess. One observation, a wind of 270 degrees at 76 knots at Halifax, Nova Scotia, was permanently discarded by the buddy system check.

In general, there is rather good agreement between the observed and analyzed winds. The wind shear lines over the Great Lakes, from North Dakota southward, and from western Tennessee southward are well depicted. However, heavy smoothing on the final analyzed fields appears to have reduced the variability in the wind speed somewhat more than desired.

SURFACE TEMPERATURE ANALYSIS

In application of the basic program to the analysis of surface temperature, five data passes are made. The radius of influence is 14.0, 14.0, 5.0, 2.5, and 1.0 grid interval for scans 1 through 5, respectively. A type 2 correction is employed on passes 1 and 2, and a type 3 correction is used on the other three scans.

The extra data pass and the rather large influence radii on the first two passes reflect an attempt to smooth unrealistic, high values of the first guess field (PE 1000 mb. temperature forecast) over the Gulf of Mexico. This problem seems to have been alleviated recently by a change in the initialization procedure for determining the boundary layer temperature (Stackpole 1969). Therefore, the extra data pass and the large influence radii may no longer be needed.

The values of ER2 and ER3 that seem to work reasonably well are both 12° F/ grid unit. The values of ER1 used on each pass are, respectively, 28.0, 27.0, 21.0, 13.5, and 11.2° F.

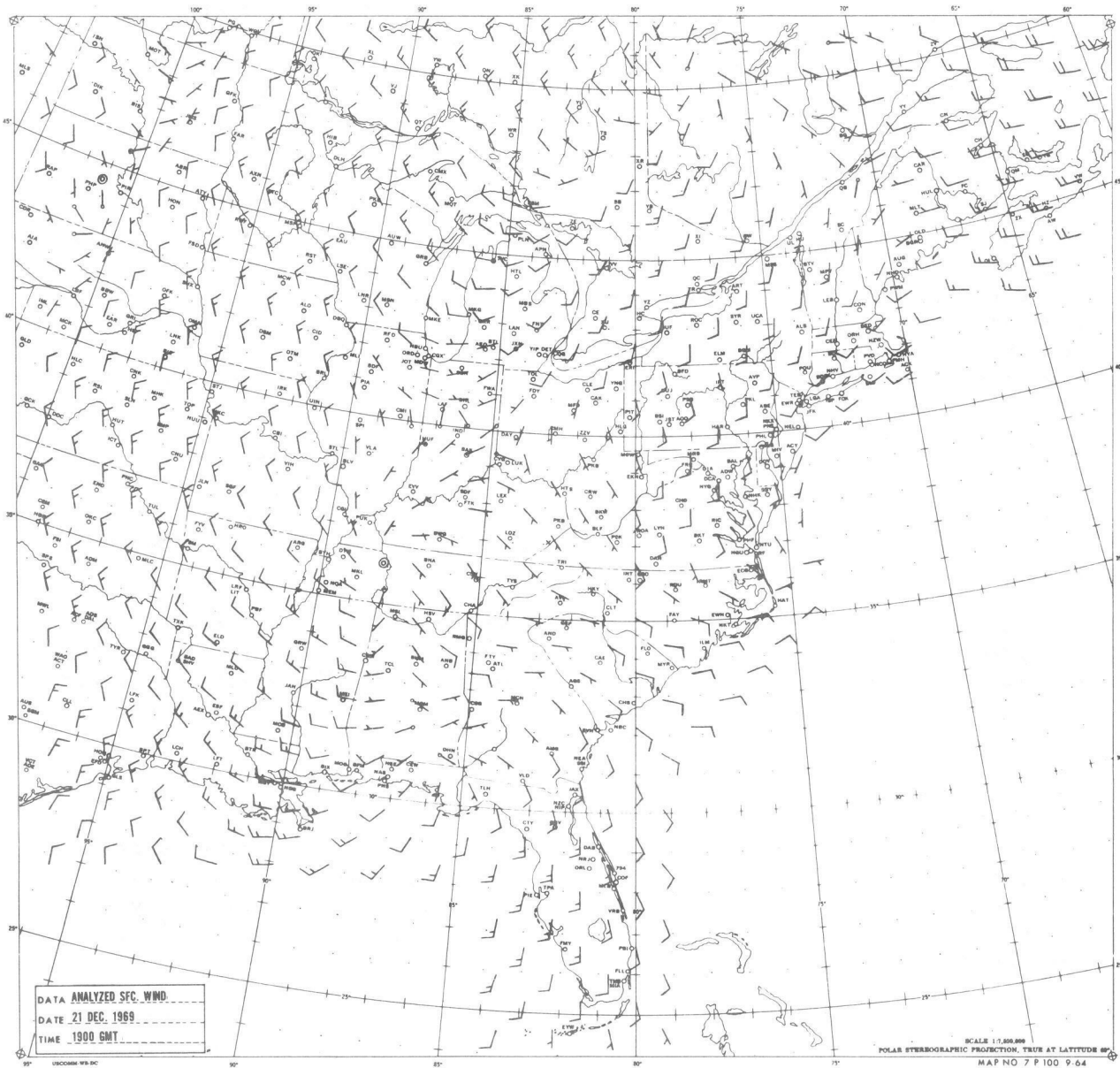


Figure 2.--The analyzed surface winds for 1900 GMT 21 December 1969, plotted at gridpoints. Symbols have their customary meaning: two concentric circles indicate calm, a shaft with no barbs indicates a speed of 1 to 2 knots, a half barb indicates a speed of 3 to 7 knots, a full barb indicates a speed of 8 to 12 knots, a full and half barb combination indicates a speed of 13 to 17 knots, etc.

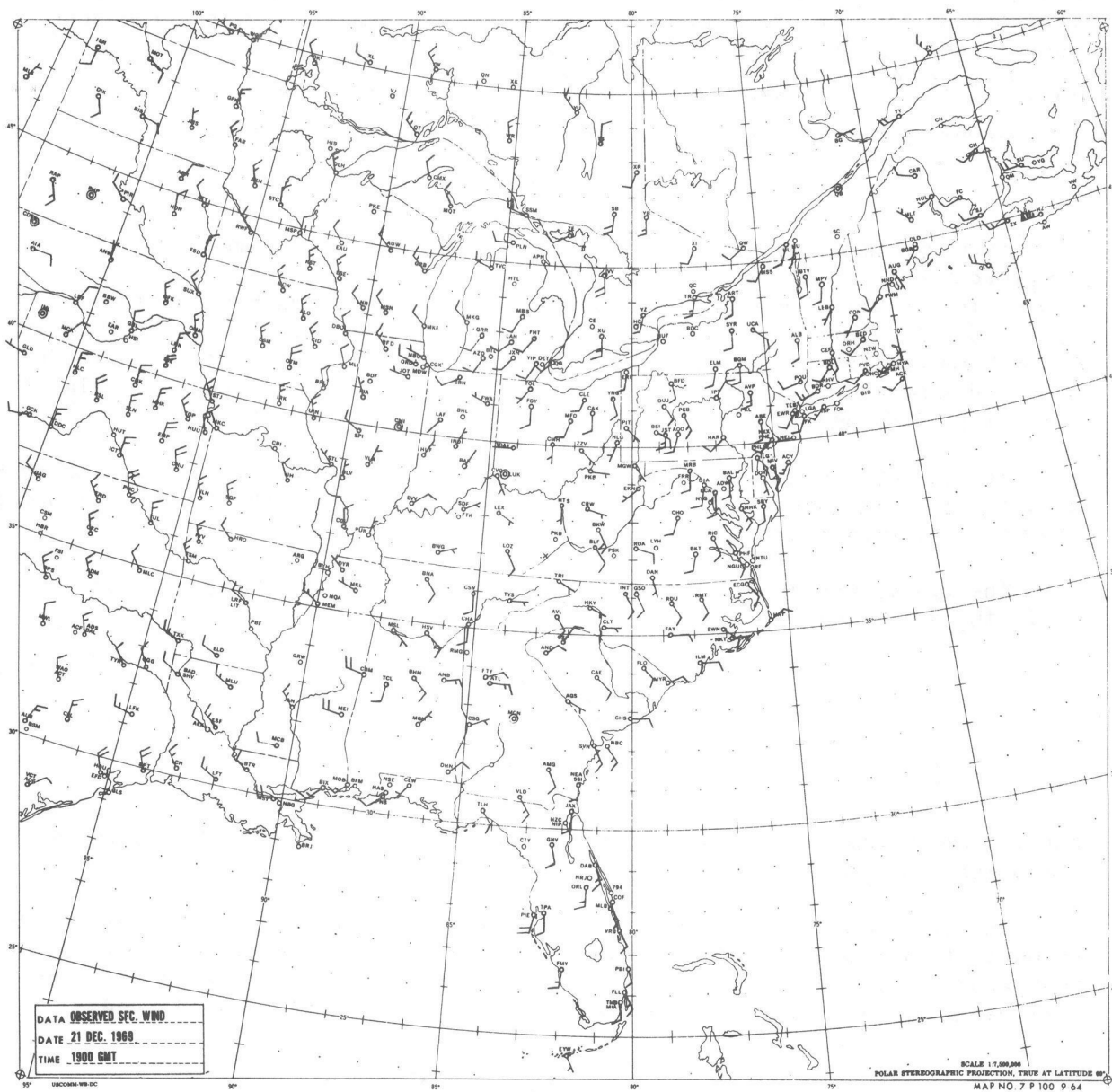


Figure 3.--The observed surface winds for 1900 GMT 21 December 1969, plotted at stations. Symbols have the same meaning as in Figure 2.

No smoothing is done at the conclusion of the first two passes. The smoothing parameter has the values 5.0, 1.0, and 5.0, respectively, on passes 3 to 5. As in the wind analysis, the smoother is applied to the analyzed field three times at the end of pass 3. Two applications of the smoother appear adequate to remove the local variability from the temperature analysis at the conclusion of pass 5.

An example of a temperature analysis is shown in figure 4.

DIAGNOSTIC COMPUTATIONS

Although objective analyses may be of some use if relayed frequently to the forecaster, their value is likely to be enhanced if fields derived kinematically from them, and relatable to significant weather, could also be supplied. In this way, any degree of development or decay could be readily determined and perhaps extrapolated into the future. The kinematic fields computed from the wind and temperature analyses are the divergence, relative vorticity, frontogenetical function, and temperature advection.

The computational area and gridlength employed here are the same as that used for the analyses. All derivatives are calculated with the usual 3 point finite difference approximation.

The divergence D and the relative vorticity ζ are computed from the following equations:

$$D = \frac{\partial u}{\partial x} + \frac{\partial v}{\partial y}$$

$$\zeta = \frac{\partial v}{\partial x} - \frac{\partial u}{\partial y}.$$

Here, u and v are the eastward (increasing x) and northward (increasing y) components of the wind vector, respectively.

The frontogenetical function F (Haltiner and Martin, 1957) as used here attempts to measure the tendency of the isotherms to pack (frontogenesis) or move apart (frontolysis) on a horizontal surface. It is computed with the following equation under the assumption that temperature is conserved:

$$F = -N_{\tau} \cdot \left(\frac{\partial T}{\partial x} \nabla u + \frac{\partial T}{\partial y} \nabla v \right).$$

Here, T is the surface temperature, ∇ is the horizontal del operator, and N_{τ} is a unit vector in the direction of ∇T . Positive values of F indicate frontogenesis, negative values, frontolysis. For the horizontal wind field considered here, only divergence and deformation can contribute to frontogenesis or frontolysis.

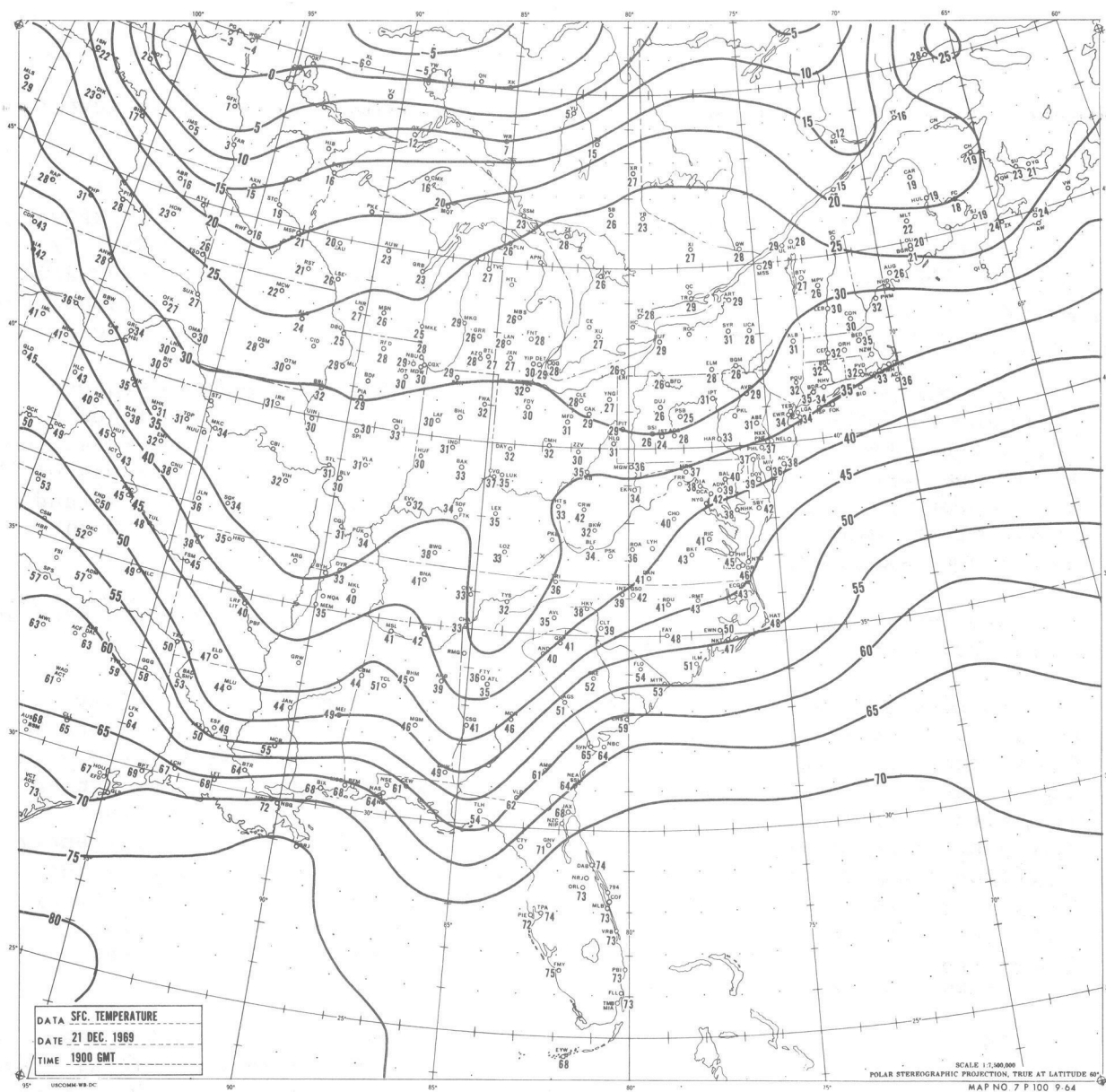


Figure 4.--The observed surface temperature and analyzed isotherms for 1900 GMT 21 December 1969. Temperatures are given in degrees Fahrenheit.

The temperature advection A is calculated by making use of the following equation:

$$A = -\left(u \frac{\partial T}{\partial x} + v \frac{\partial T}{\partial y}\right).$$

Positive values of A indicate warm advection, negative values, cold advection.

RESULTS OF COMPUTATIONS

For the purpose of the ensuing discussion, the NMC sea level pressure and frontal analysis for 0600 GMT, 21 December 1969, and for 1800 GMT, 21 December 1969, are shown in figures 5 and 6, respectively. The shaded areas denote precipitation occurring at map time. All diagnostic computations were made from analyses of observations taken one hour after these map times.

The divergence, vorticity, frontogenetical function, and temperature advection for 0700 GMT and 1900 GMT are shown in figures 7-10 and figures 11-14, respectively. The frontogenetical function and temperature advection fields have been smoothed once with $b = 5.0$ after computation. Because of the heavy smoothing of the analyzed fields, it can be seen that the maxima and minima of the diagnostic fields do not have the extreme values that might normally be expected.

The results and accompanying remarks for the two cases presented here are, in general, applicable to 15 other cases which were examined.

At 0700 GMT, a warm front (figure 5) extends from an incipient wave cyclone in east Texas to the Gulf of Mexico. A trough extends northward to Canada from the Texas cyclone. Widespread precipitation is associated with these systems. The divergence field for 0700 GMT (figure 7) agrees rather well with these features. Of further interest is the area of negative divergence (convergence) over the lower Mississippi River, where apparently organized thunderstorms were observed. This is also well depicted by the cyclonic vorticity in the vorticity field (figure 8). In a previous study which made use of hourly surface data, Endlich and Mancuso (1967) also demonstrated the proximity of organized thunderstorm activity to areas of surface convergence and cyclonic vorticity.

The frontogenetical function for 0700 GMT (figure 9), indicates weak frontogenesis taking place in the frontal zone over Louisiana and Texas. Weak to moderate warm advection over this area is indicated in figure 10. There does not appear to be any direct indication of the thunderstorm activity in the field of frontogenetical function.

Petterssen and Austin (1942) have shown that, in general, frontal intensity (isotherm concentration) is related to the magnitude of the vorticity at the front. This relationship is demonstrated to some extent by the trough oriented north to south from Canada to Texas. The temperature gradient field at this time (not shown) indicates that the weakest gradient is found over central Kansas. The vorticity field (figure 8), shows the weakest cyclonic vorticity to be over southern Kansas and northern Oklahoma.

The axis of maximum vorticity should, of course, locate the position of a front. Although the trough over the plains is weak, the vorticity does indicate the position well. An exception is the cyclonic area over northern Minnesota which is not related to any front. In addition, the warm front over central Louisiana is not depicted well. This is due to the overriding cyclonic vorticity center over the Mississippi River associated with the thunderstorm activity.

Figure 6, the NMC surface chart 12 hours later, shows two rather broad low pressure areas, one along the northern border of Mississippi and Alabama which is occluding, and the other north of Lake Huron. Although the centers of these lows are not accurately located by the analyzed wind field (figure 2), they are represented quite well by the divergence and vorticity fields (figures 11 and 12, respectively).

Of significance is the warm frontal development over the southeastern part of the United States. This feature is clearly indicated in a comparison of the magnitudes of the kinematically derived fields at 1900 GMT (figures 11-14) with those of the 0700 GMT fields (figures 7-10). Associated with the warm front are thunderstorms in the western panhandle region of Florida and in southeastern Alabama. In addition, three tornadoes were reported approximately 40 miles west of Tallahassee, Florida, at about 1900 GMT. Centers of convergence and cyclonic vorticity are close to this area of thunderstorm and tornado activity. The frontogenesis in this active region is also illustrated in figure 13, as is the proximity of an area of relatively high values of warm advection in figure 14.

It is of interest to note the temperature advection field (figure 14) in the vicinity of the occluding low pressure area. As expected, cold advection precedes and follows this occluding cyclone, with only a very weak tongue of warm advection between. It is not surprising that the cyclone continued to decay.

A further comparison of figures 11-14 and figures 7-10 also shows the development occurring north of Lake Huron. An approximate threefold increase in the magnitude of the temperature gradient has occurred in this region during the 12 hour period. This increase in frontal intensity, which is shown in the field of frontogenetical function (figure 13), is also well indicated by the increase of cyclonic vorticity, as illustrated by comparing figures 8 and 12. This is a good illustration of the relationship between frontal intensity and vorticity. The convergent wind field (figure 11), which tends to pack the isotherms, contributes to the increase of cyclonic vorticity.

An interesting feature regarding the general development in the 12 hour period is brought out by comparing the temperature advection charts for 0700 GMT and 1900 GMT (figures 10 and 14, respectively). A definite increase in the cold advection to the rear of the trough north of Lake Huron is noted; however, no change is noted in the weak warm advection preceding it.

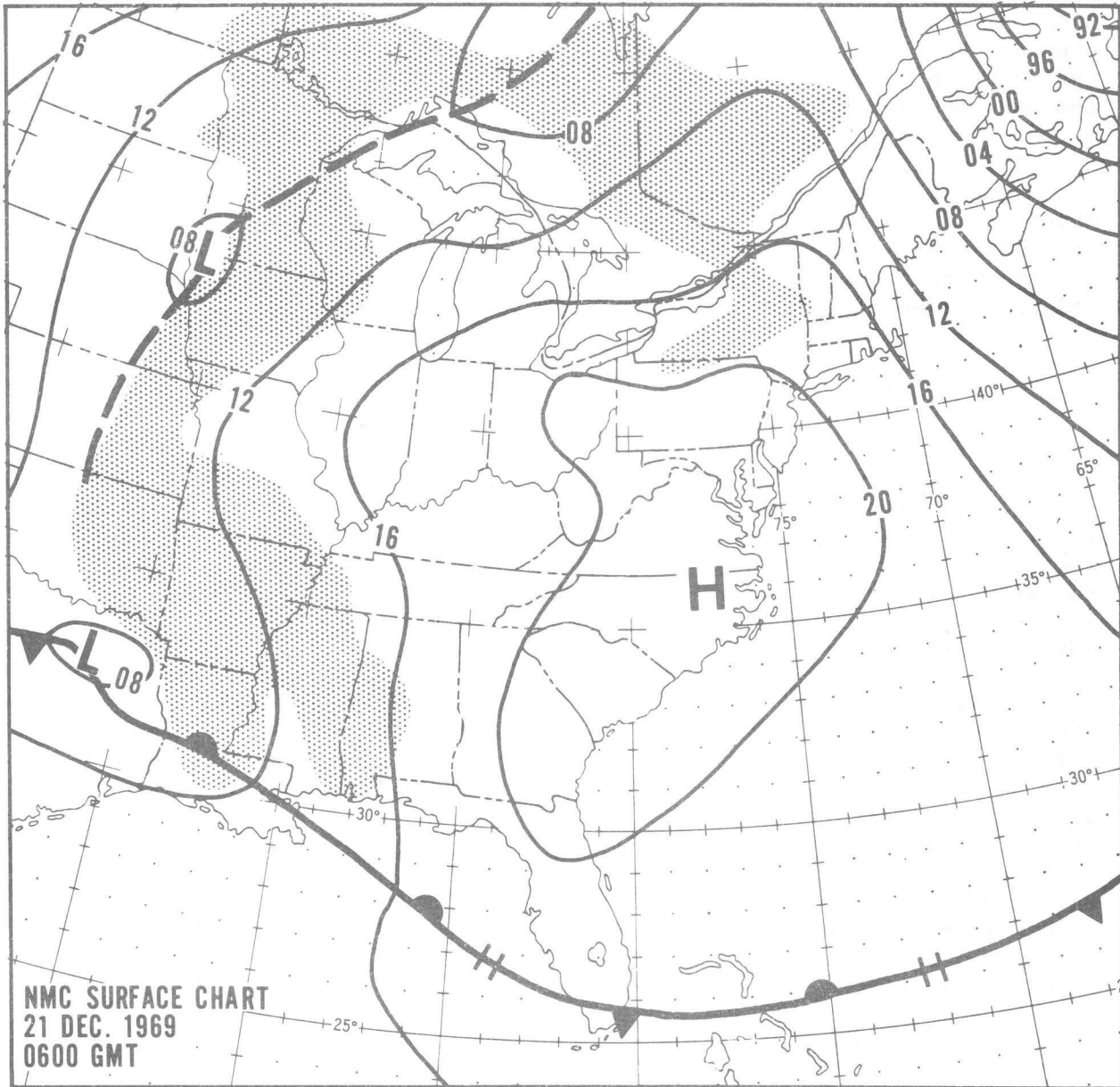


Figure 5.--The NMC sea level pressure and frontal analysis for 0600 GMT
21 December 1969.

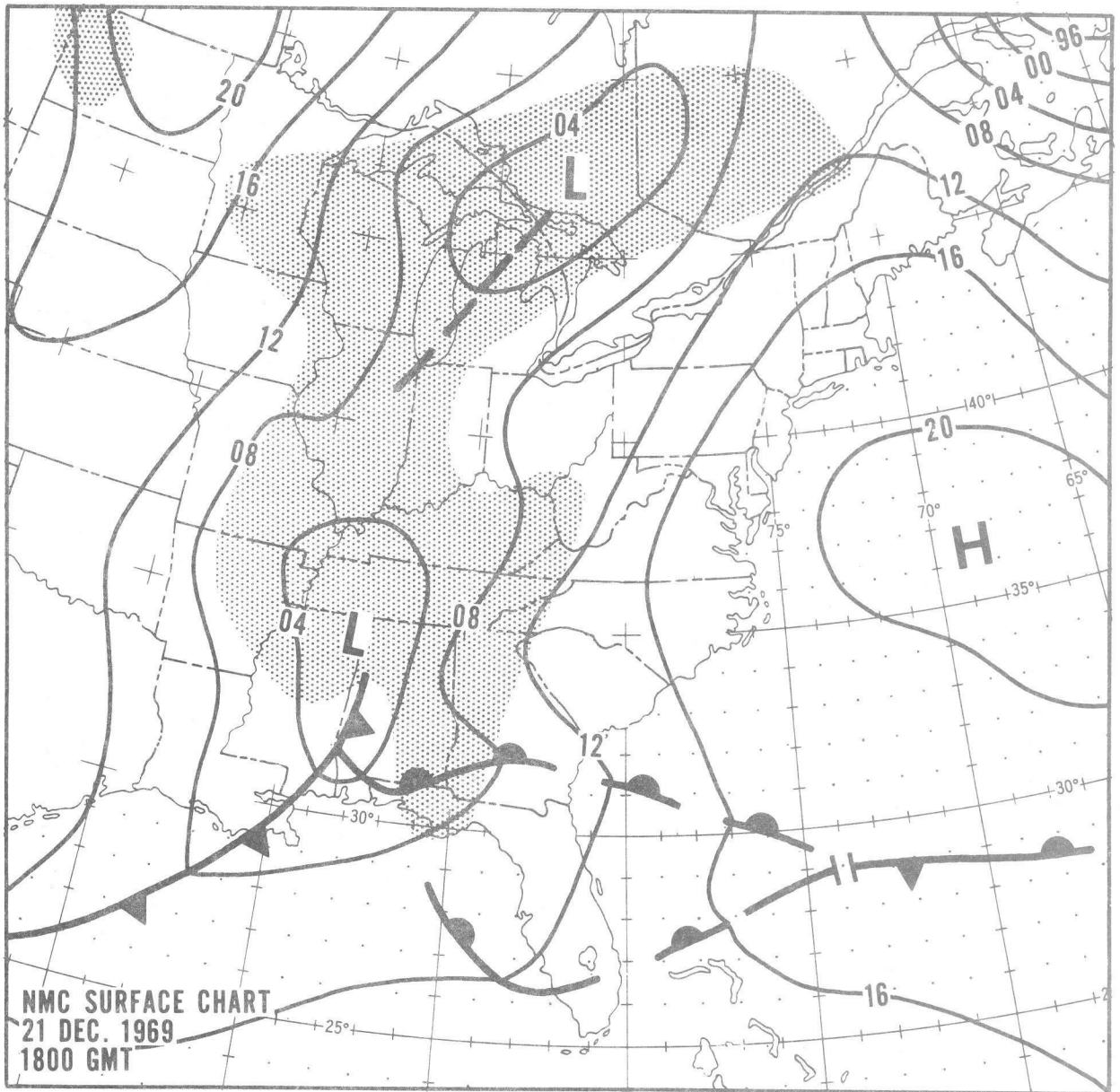


Figure 6.--The NMC sea level pressure and frontal analysis for 1800 GMT
21 December 1969.

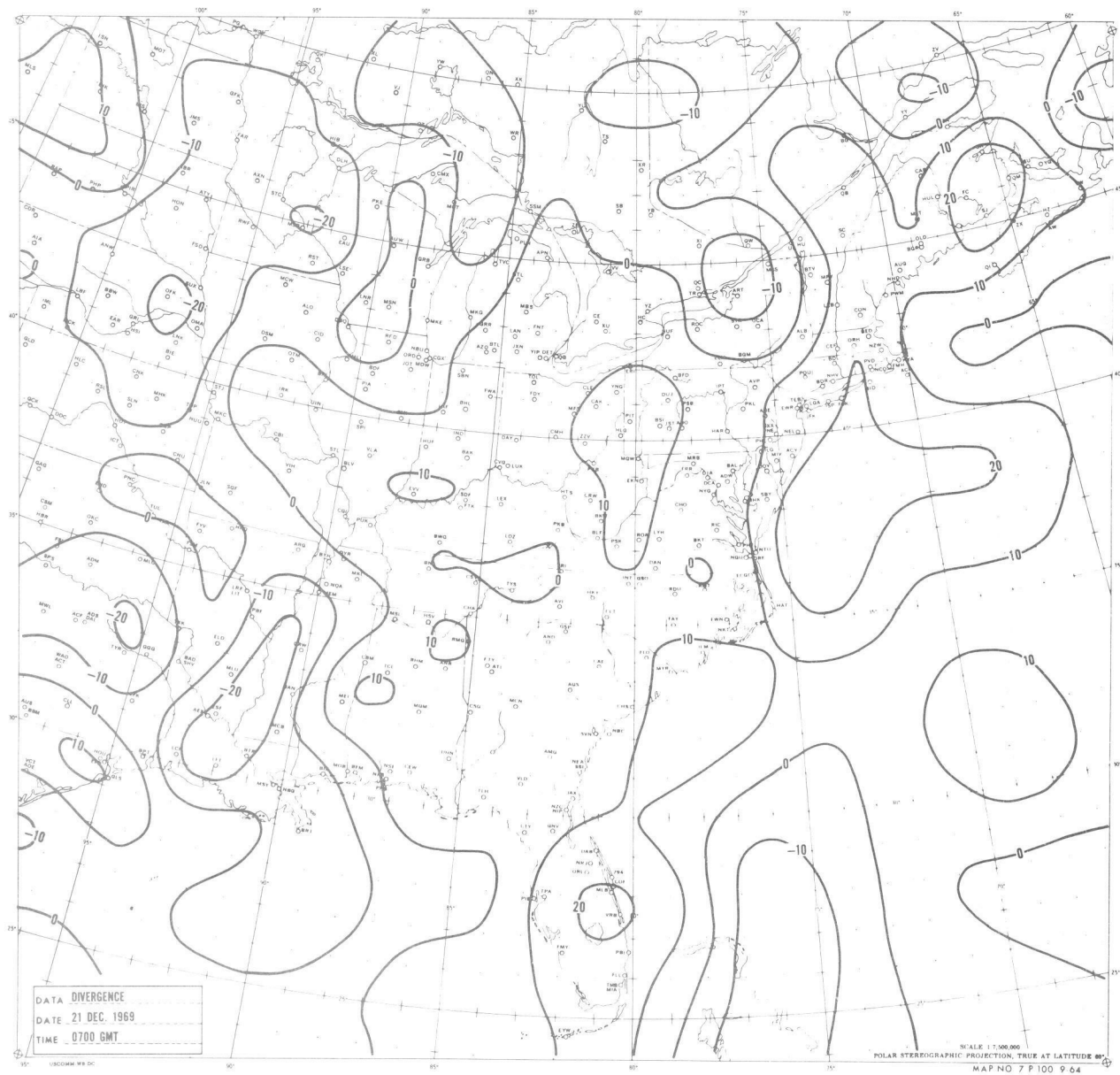


Figure 7.--The field of surface divergence for 0700 GMT 21 December 1969. Values are in units 10^{-6} sec^{-1} . Negative values indicate convergence.

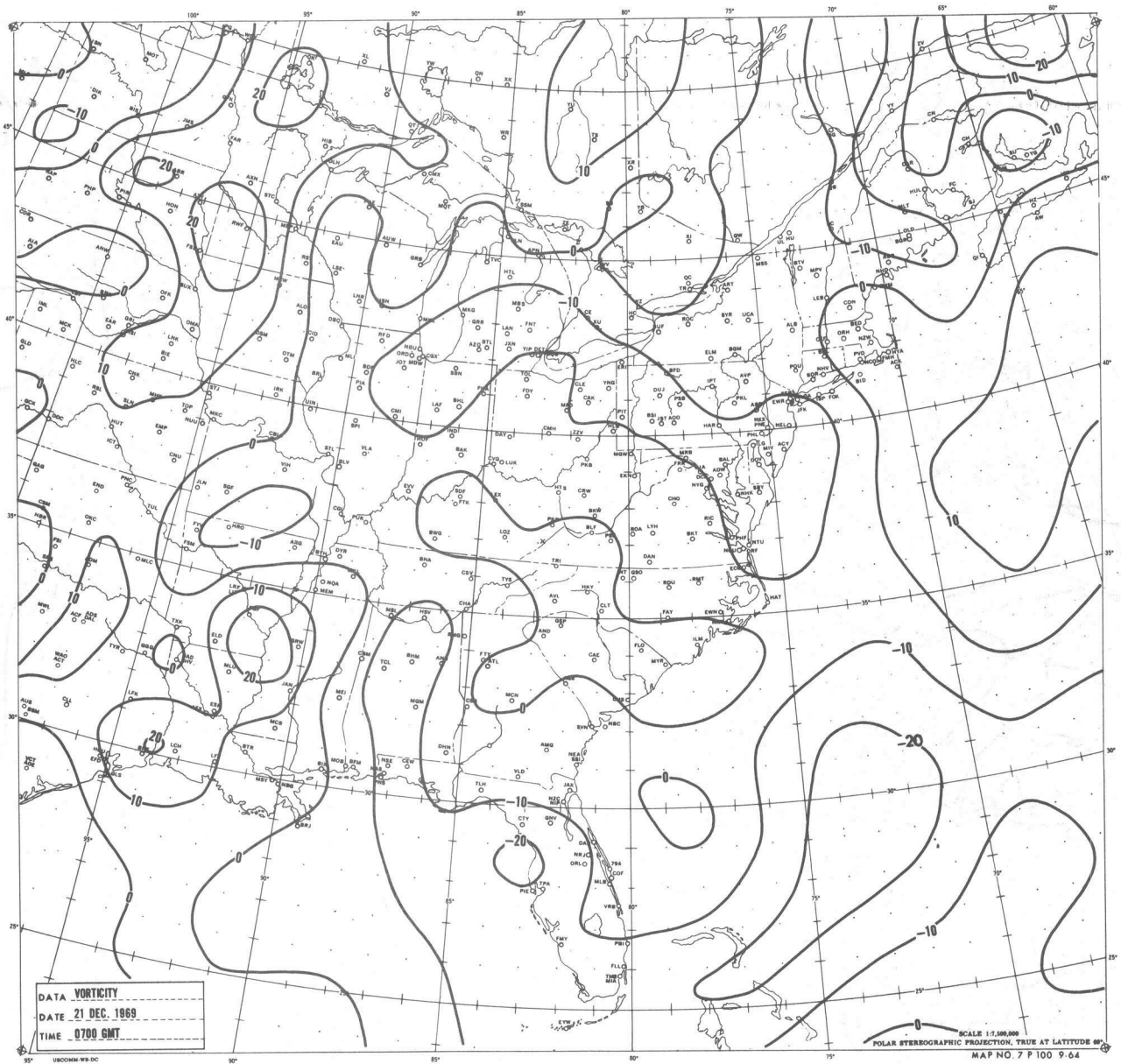


Figure 8.--The field of surface vorticity for 0700 GMT 21 December 1969. Values are in units 10^{-6} sec^{-1} . Positive values indicate cyclonic vorticity.

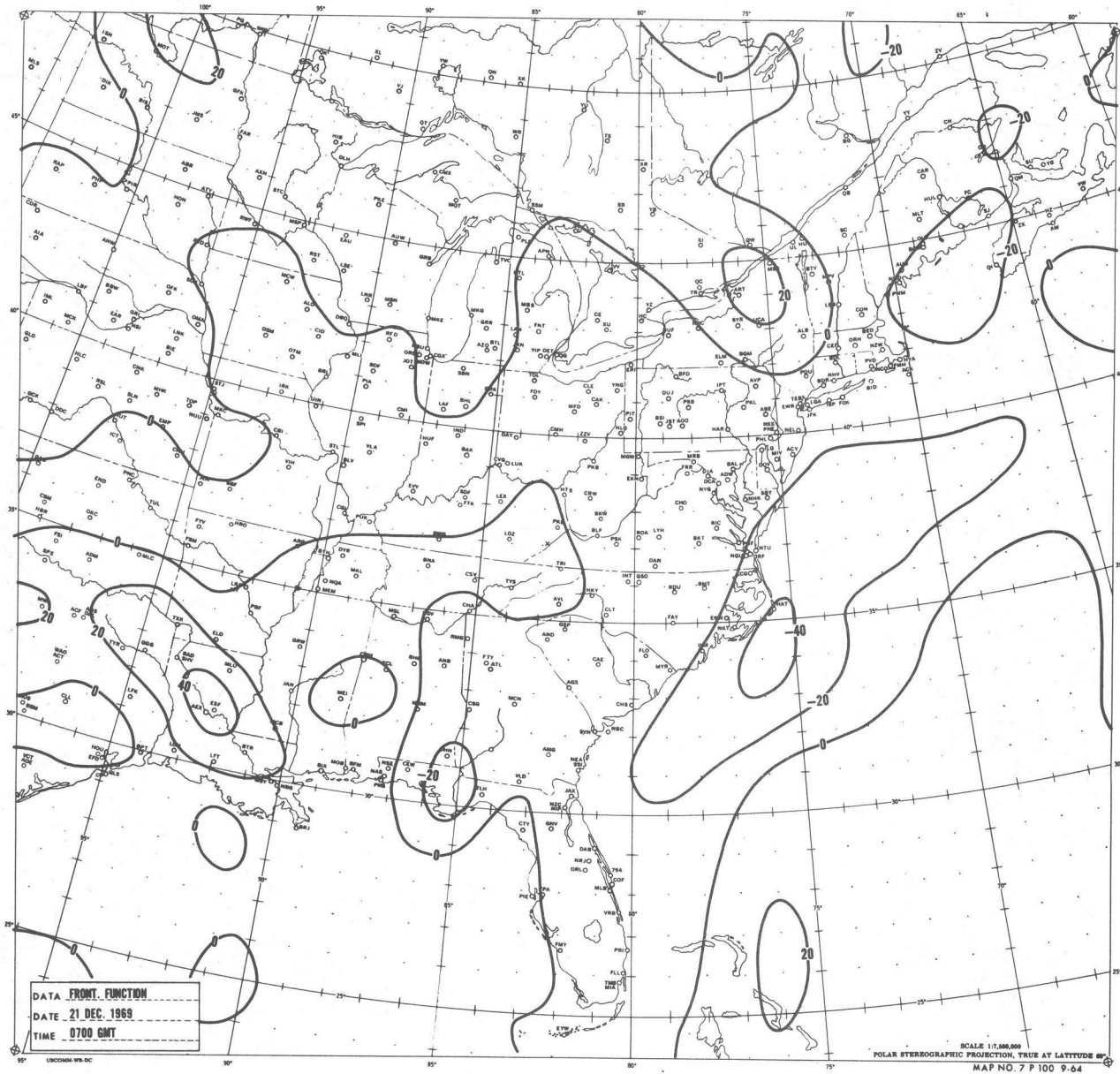


Figure 9.--The field of frontogenetical function for 0700 GMT 21 December 1969. Values are in units $10^{-11} \text{ deg.C(m.sec)}^{-1}$.

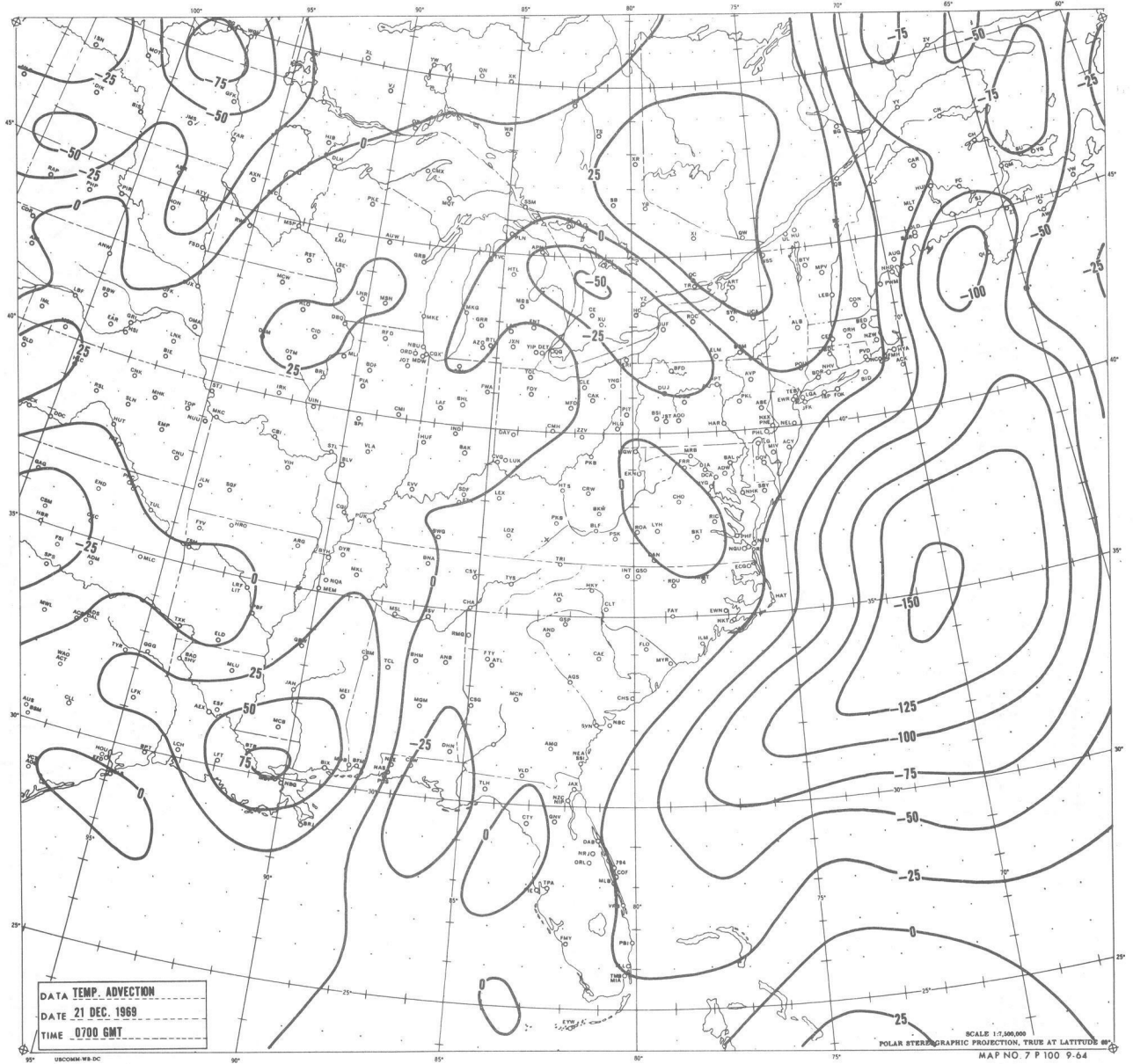


Figure 10.--The field of temperature advection for 0700 GMT 21 December 1969. Values are in units 10^{-2} deg.F(hr.) $^{-1}$.

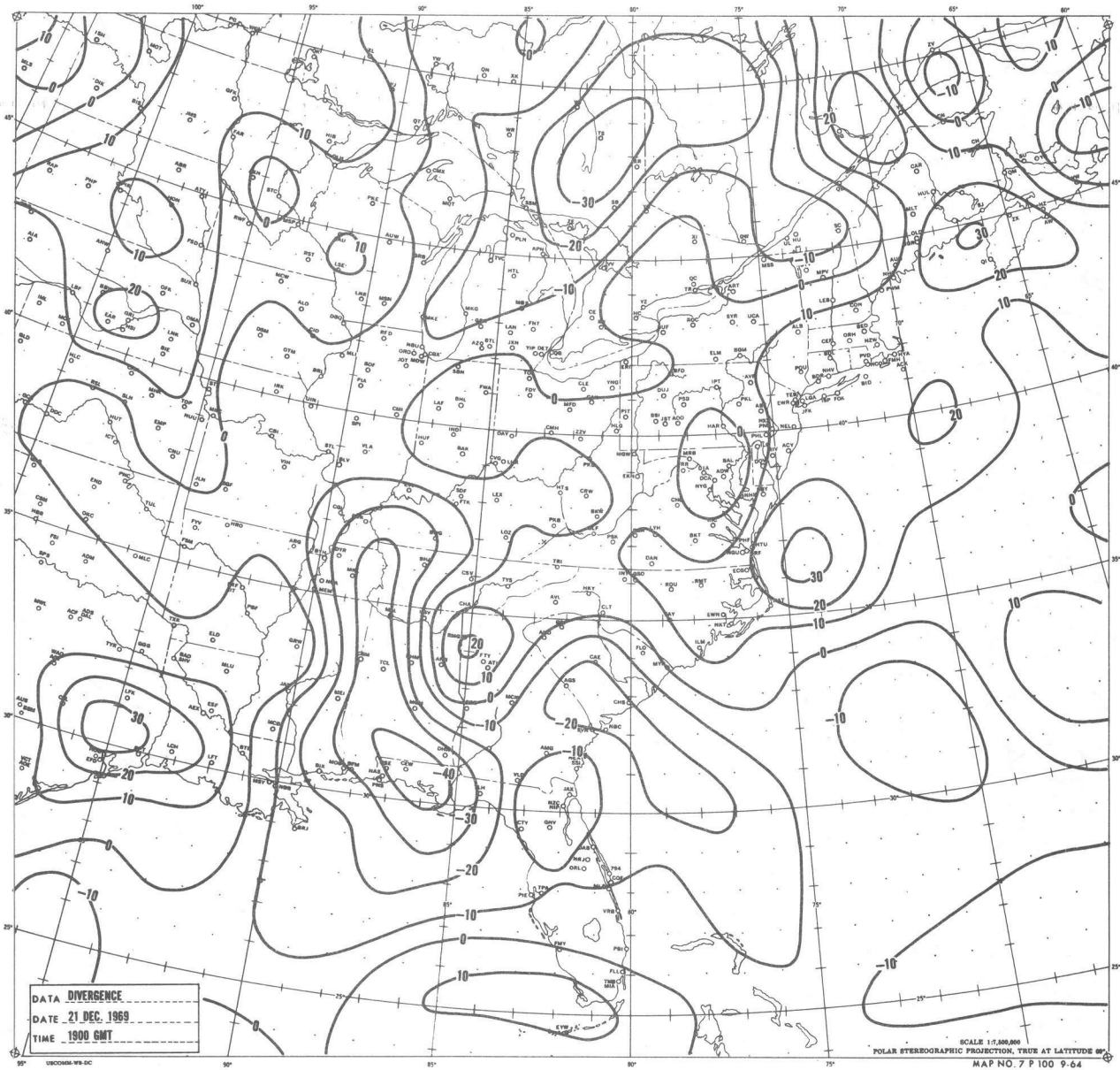


Figure 11.--The field of surface divergence for 1900 GMT 21 December 1969.
Values have the same units as in Figure 7.

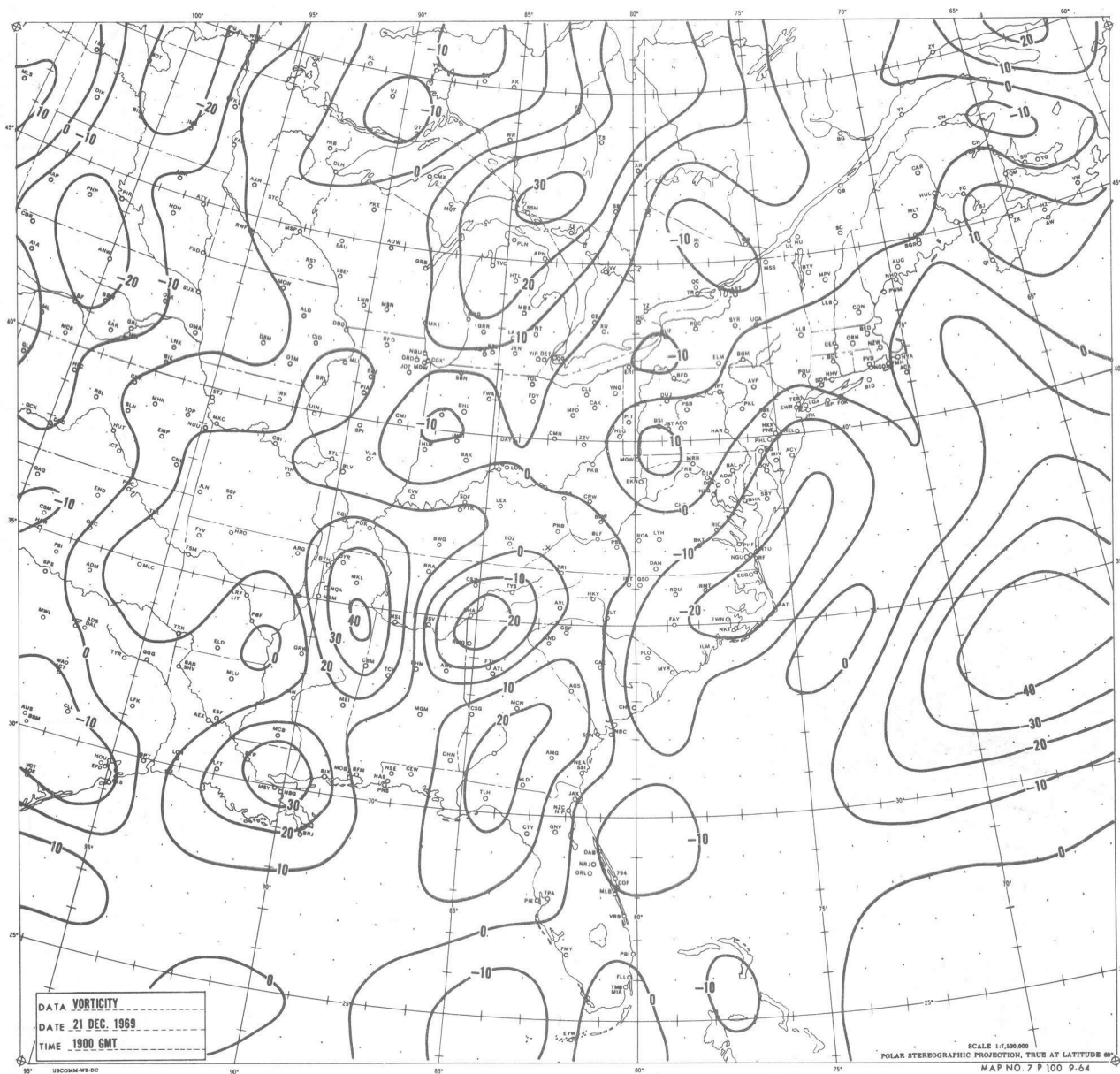


Figure 12.--The field of surface vorticity for 1900 GMT 21 December 1969.
 Values have the same units as in Figure 8.

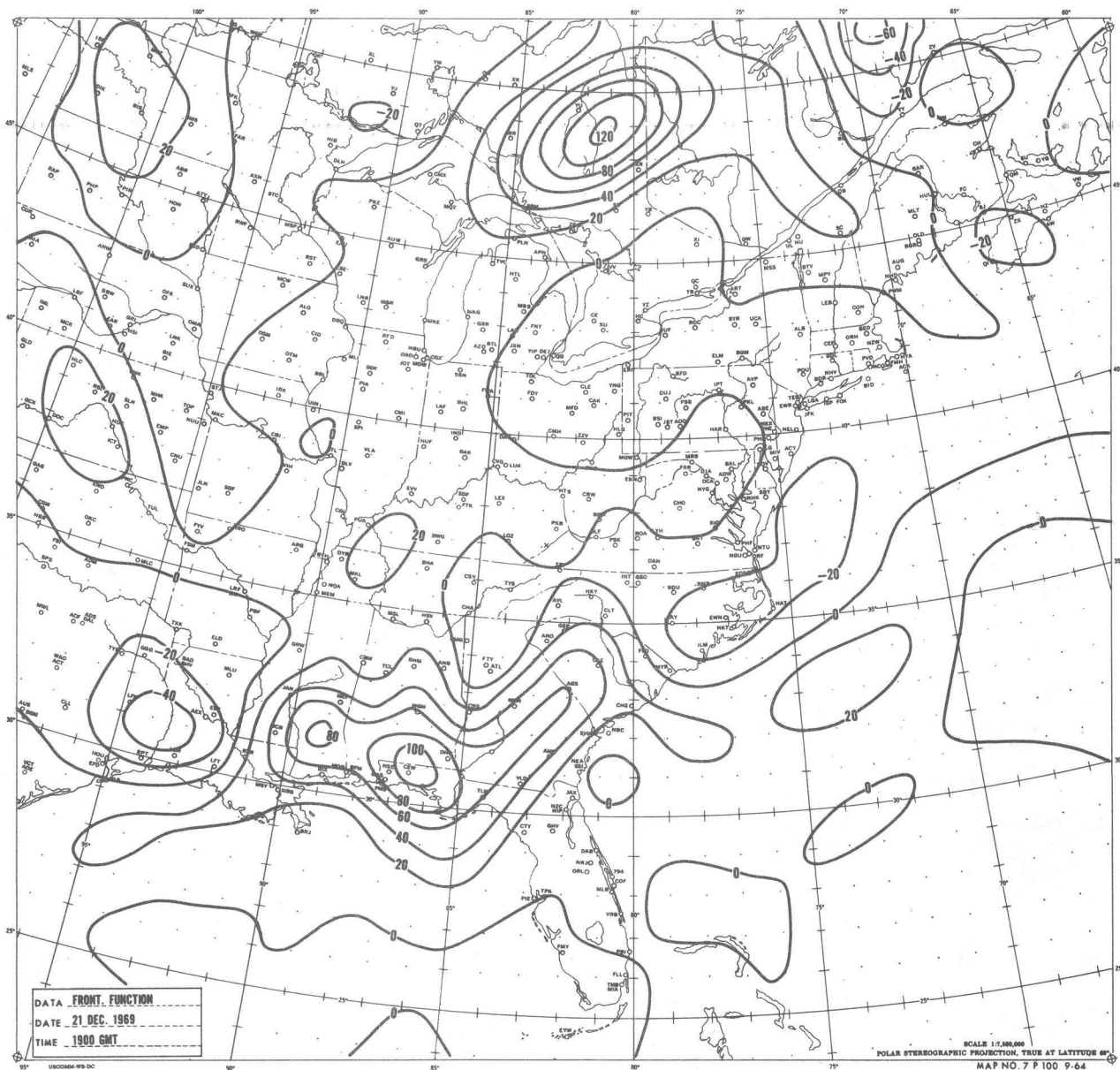


Figure 13.--The field of frontogenetical function for 1900 GMT 21 December 1969. Values have the same units as in Figure 9.

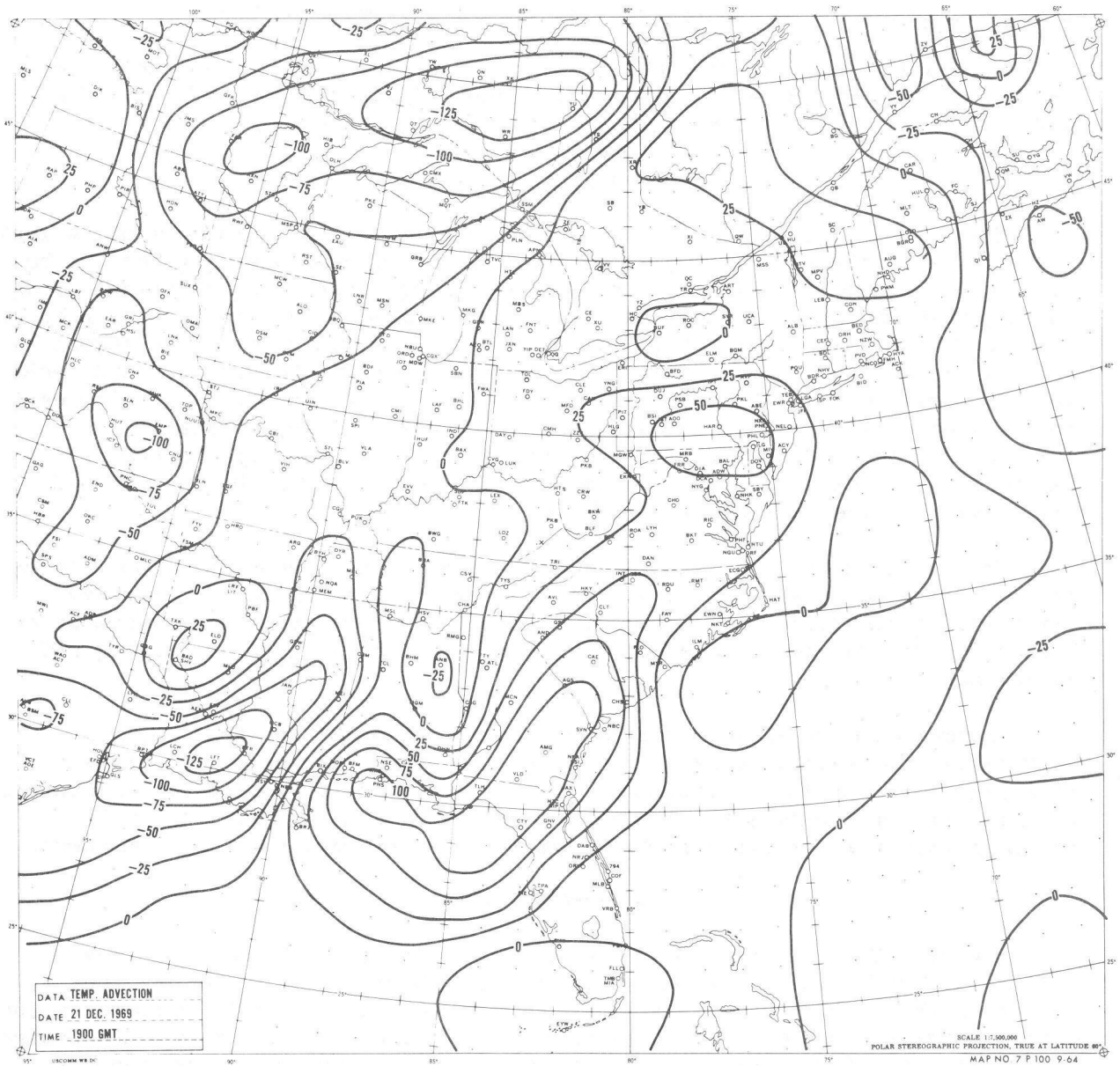


Figure 14.--The field of temperature advection for 1900 GMT 21 December 1969. Values have the same units as in Figure 10.

As the temperature advection and the other 1900 GMT surface fields may indicate, significant development in the following 12 hours took place on the warm front over the southeastern part of the United States; no further development occurred north of the Great Lakes during this time period.

As was the case at 0700 GMT, the axis of maximum vorticity in the vorticity field at 1900 GMT (figure 12) also identifies the position of the fronts and troughs quite satisfactorily.

SUMMARY AND CONCLUSIONS

The hourly surface temperature and wind observations have been objectively analyzed in an attempt to compute diagnostic fields which can provide information not normally available for use in short range weather predictions. Both the analyses and computations have been performed on a relatively fine grid so that smaller scale features might be maintained. Because of rather strong local variability of the wind and temperature observations, these fields were heavily smoothed. Nevertheless, the remaining product seems, in some cases, to relate to smaller scale features such as regions of thunderstorm and tornado activity and incipient cyclogenesis. In addition, the location, intensity, and related weather of frontal systems appear to be represented rather well by one or more of the diagnostic fields.

Of all the diagnostic fields, the frontogenetical function appears to be open to the most question. It is not readily apparent if it contains any additional information about frontal intensity and development that cannot be inferred from the other diagnostic fields, in particular, the vorticity and divergence.

Although the diagnostic fields appear to be useful in short range prediction, their true value can only be determined through a limited test on a regularly scheduled basis at a weather station with access to a computer. In this way, the usefulness of the analyses and diagnostic fields can be properly evaluated by experienced forecasters in an operational environment.

ACKNOWLEDGMENTS

I would like to extend my appreciation to Dr. Harry R. Glahn of the Techniques Development Laboratory for his very helpful advice during the course of this work. I would also like to thank Mr. Charles F. Roberts of the Forest Service, who provided the initial suggestion for this study, Mr. George W. Hollenbaugh of the Techniques Development Laboratory, who furnished the original automatic decoding and analysis programs, and Mrs. Rosina C. Lopresti who prepared the manuscript for printing.

REFERENCES

- Bergthorssen, P., and B. R. Döös, "Numerical Weather Map Analysis," Tellus, Vol. 7, No. 3, August 1955, pp. 329-340.
- Cressman, G. P., "An Operational Objective Analysis System," Monthly Weather Review, Vol. 87, No. 10, October 1959, pp. 367-374.
- Endlich, R. M., and R. L. Mancuso, "Environmental Conditions Associated with Severe Thunderstorms and Tornadoes," Final Report, Contract Cwb-11293, Stanford Research Institute, Menlo Park, Calif., May 1967, 106 pp.
- Glahn, H. R., G. W. Hollenbaugh, and D. A. Lowry, "An Operationally Oriented Objective Analysis Program," ESSA Technical Memorandum WBTM TDL-22, July 1969a, 20 pp.
- Glahn, H. R., D. A. Lowry, and G. W. Hollenbaugh, "An Operational Subsynoptic Advection Model," ESSA Technical Memorandum WBTM TDL-23, July 1969b, 26 pp.
- Haltiner, G. J., and F. L. Martin, Dynamical and Physical Meteorology, McGraw-Hill Book Company, Inc., New York, 1957, pp. 287-296.
- Hollenbaugh, G. W., H. R. Glahn, and D. A. Lowry, "Automatic Decoding of Hourly Weather Reports," ESSA Technical Memorandum WBTM TDL-21, July 1969, 27 pp.
- Petterssen, S., and J. M. Austin, "Fronts and Frontogenesis in Relation to Vorticity," Papers in Physical Oceanography and Meteorology, Vol. 7, No. 2, January 1942, 37 pp.
- Reap, R. M., "Prediction of Temperature and Dew Point by Three-Dimensional Trajectories," ESSA Technical Memorandum WBTM TDL-15, October 1968, 20 pp.
- Shuman, F. G., and J. B. Hovermale, "An Operational Six-Layer Primitive Equation Model," Journal of Applied Meteorology, Vol. 7, No. 4, August 1968, pp. 525-547.
- Stackpole, J. D., "Changes in Initialization Procedures for Boundary Layer Temperatures," Technical Procedures Bulletin No. 34, ESSA, Weather Bureau, October 1969, 2 pp.

(Continued from inside front cover)

- WBTM TDL 16 Objective Visibility Forecasting Techniques Based on Surface and Tower Observations. Donald M. Gales, October 1968. (PB-180 479)
- WBTM TDL 17 Second Interim Report on Sea and Swell Forecasting. N. A. Pore and Lt. W. S. Richardson, USESSA, January 1969. (PB-182 273)
- WBTM TDL 18 Conditional Probabilities of Precipitation Amounts in the Conterminous United States. Donald L. Jorgensen, William H. Klein, and Charles F. Roberts, March 1969. (PB-183 144)
- WBTM TDL 19 An Operationally Oriented Small-Scale 500-Millibar Height Analysis. Harry R. Glahn and George W. Hollenbaugh, March 1969. (PB-184 111)
- WBTM TDL 20 A Comparison of Two Methods of Reducing Truncation Error. Robert J. Bermowitz, May 1969. (PB-184 741)
- WBTM TDL 21 Automatic Decoding of Hourly Weather Reports. George W. Hollenbaugh, Harry R. Glahn, and Dale A. Lowry, July 1969. (PB-185 806)
- WBTM TDL 22 An Operationally Oriented Objective Analysis Program. Harry R. Glahn, George W. Hollenbaugh, and Dale A. Lowry, July 1969. (PB-186 129)
- WBTM TDL 23 An Operational Subsynoptic Advection Model. Harry R. Glahn, Dale A. Lowry, and George W. Hollenbaugh, July 1969. (PB-186 389)
- WBTM TDL 24 A Lake Erie Storm Surge Forecasting Technique. William S. Richardson and N. Arthur Pore, August 1969. (PB-185 778)
- WBTM TDL 25 Charts Giving Station Precipitation in the Plateau States From 850- and 500-Millibar Lows During Winter. August F. Korte, Donald L. Jorgensen, and William H. Klein, September 1969. (PB-187 476)
- WBTM TDL 26 Computer Forecasts of Maximum and Minimum Surface Temperatures. William H. Klein, Frank Lewis, and George P. Casely, October 1969. (PB-189 105)
- WBTM TDL 27 An Operational Method for Objectively Forecasting Probability of Precipitation. Harry R. Glahn and Dale A. Lowry, October 1969. (PB-188 660)
- WBTM TDL 28 Techniques for Forecasting Low Water Occurrences at Baltimore and Norfolk. Lt. (jg) James M. McClelland, USESSA, March 1970. (PB-191 744)
- WBTM TDL 29 A Method for Predicting Surface Winds. Harry R. Glahn, March 1970. (PB-191 745)
- WBTM TDL 30 Summary of Selected Reference Material on the Oceanographic Phenomena of Tides, Storm Surges, Waves, and Breakers. Arthur N. Pore, May 1970. (PB-193 449)
- WBTM TDL 31 Persistence of Precipitation at 108 Cities in the Conterminous United States. Donald L. Jorgensen and William H. Klein, May 1970. (PB-193 599)
- WBTM TDL 32 Computer-Produced Worded Forecasts. Harry R. Glahn, June 1970. (PB-194 262)
- WBTM TDL 33 Calculation of Precipitable Water. L. P. Harrison, June 1970. (PB-193 600)
- WBTM TDL 34 An Objective Method for Forecasting Winds Over Lake Erie and Lake Ontario. Celso S. Barrientos, August 1970. (PB-194 586)
- WBTM TDL 35 A Probabilistic Prediction in Meteorology: A Bibliography. A. H. Murphy and R. A. Allen, June 1970. (PB-194 415)
- WBTM TDL 36 Current High Altitude Observations--Investigation and Possible Improvement. M. A. Alaka and R. C. Elvander, July 1970. (Com-71-00003)
- NWS TDL 37 Prediction of Surface Dew Point Temperatures. R. C. Elvander, January 1971.



100-100-100



100-100-100